Cell Reports
Article



# Trpc2-Expressing Sensory Neurons in the Main Olfactory Epithelium of the Mouse

Masayo Omura[1] and Peter Mombaerts[1,*]
[1]Max Planck Research Unit for Neurogenetics, 60438 Frankfurt, Germany
*Correspondence: peter.mombaerts@biophys.mpg.de
http://dx.doi.org/10.1016/j.celrep.2014.06.010


## SUMMARY

**The mouse olfactory system contains two distinct chemosensory epithelia, the main olfactory epithelium (MOE) and the vomeronasal epithelium (VNE). Their sensory neurons express odorant receptor genes and vomeronasal receptor genes, respectively, and differ fundamentally in their signal transduction pathways. Genes required for chemosensory transduction are the cyclic nucleotide-gated channel subunit *Cnga2* and the transient receptor potential cation channel *Trpc2*, respectively. Here, we document two previously unrecognized types of Trpc2+ neurons in the MOE of mice of various ages, including adults. These cell types express *Cnga2* and can be distinguished by expression of adenylate cyclase *Adcy3* (positive: type A; negative: type B). A third of MOE neurons that express the odorant receptor genes *Olfr68*/*Olfr69* coexpress *Trpc2* and are type A cells. In Trpc2-IRES-taulacZ gene-targeted mice, some labeled axons coalesce into glomeruli in the main olfactory bulb. Our findings have implications for the conventional VNE-centric interpretation of the behavioral phenotypes of Trpc2 knockout mice.**

## INTRODUCTION

Rodents such as mice and rats rely heavily on their chemosensory senses (smell and taste). Their olfactory system can be broadly divided into the main olfactory system and the accessory or vomeronasal system. Within the main olfactory epithelium (MOE) and vomeronasal epithelium (VNE) reside olfactory sensory neurons (OSNs) and vomeronasal sensory neurons (VSNs), respectively. Their axons coalesce into glomeruli within the main olfactory bulb and the accessory olfactory bulb (AOB), respectively. The predominant neuronal cell type in the MOE expresses OR genes, a repertoire of ~1,200 G protein-coupled receptor genes; these cells are henceforth referred to as canonical OSNs. The predominant neuronal cell type in the VNE expresses two repertoires of unrelated G protein-receptor genes, the *Vmn1r* and *Vmn2r* genes. OSNs typically detect general odorants, whereas VSNs are specialized in the detection of pheromones and other chemical ligands that modulate behavior among individuals (Wyatt, 2014). The chemosensory transduction pathways differ fundamentally between OSNs and VSNs, and neuronal responses are differentially affected in Cnga2 knockout (Cnga2-KO) mice (OSNs) versus Trpc2-KO mice (VSNs). Trpc2-KO males and females display striking behavioral phenotypes: their sexual, aggressive, and parenting behaviors are profoundly perturbed (Leypold et al., 2002; Stowers et al., 2002; Kimchi et al., 2007; Wu et al., 2014). Based on the assumption of VSN-specific expression of Trpc2 in the mouse, these behavioral phenotypes have been widely interpreted in VSN-specific terms (Dulac and Torello, 2003; Dulac and Wagner, 2006; Papes et al., 2010; Fraser and Shah, 2014; Wu et al., 2014).

Surprisingly, after the pioneering discovery of Trpc2 expression in rat VSNs (Liman et al., 1999), no published study has characterized Trpc2 expression thoroughly in the olfactory system of the mouse, the species that was the subject of the gene knockout experiments. Although numerous papers have confirmed Trpc2 expression in mouse VSNs, they did not provide any analyses of the mouse MOE (Stowers et al., 2002). In the process of performing *Trpc2* in situ hybridization (ISH) in mice, we observed that some MOE cells also express *Trpc2*, and decided to pursue this unexpected finding. Here, we document Trpc2 expression in two previously unrecognized types of MOE neurons using a variety of complementary techniques, i.e., by using ISH and immunohistochemistry (IHC) with a Trpc2 polyclonal antibody (Liman et al., 1999) in wild-type (WT) C57BL/6 mice, and by expressing an axonal marker in a gene-targeted mouse strain carrying a Trpc2-IRES-taulacZ mutation. The specificity of our ISH and IHC reagents is proved by the absence of signals in Trpc2-KO mice. We distinguish two types of Trpc2+ MOE neurons on the basis of several criteria. Type A cells are *Adcy3*+ and type B cells are *Adcy3*−. In Trpc2-IRES-taulacZ mice, some Trpc2+ neurons coalesce into a few glomeruli on the ventral aspect of the main olfactory bulb near the necklace glomeruli, and this pattern is disrupted in Cnga2-KO mice. Our findings pose a challenge to the conventional VSN-specific interpretation of the behavioral phenotypes of Trpc2-KO mice.

## RESULTS

### *Trpc2* Gene Expression in the VNO and MOE of WT C57BL/6 mice

The mouse *Trpc2* gene is located ~380 kilobases (kb) centromerically from the first of >100 class I OR genes on chromosome 7. Its VSN transcript consists of 13 coding exons (Figure 1A) that encode a predicted polypeptide of 890 amino

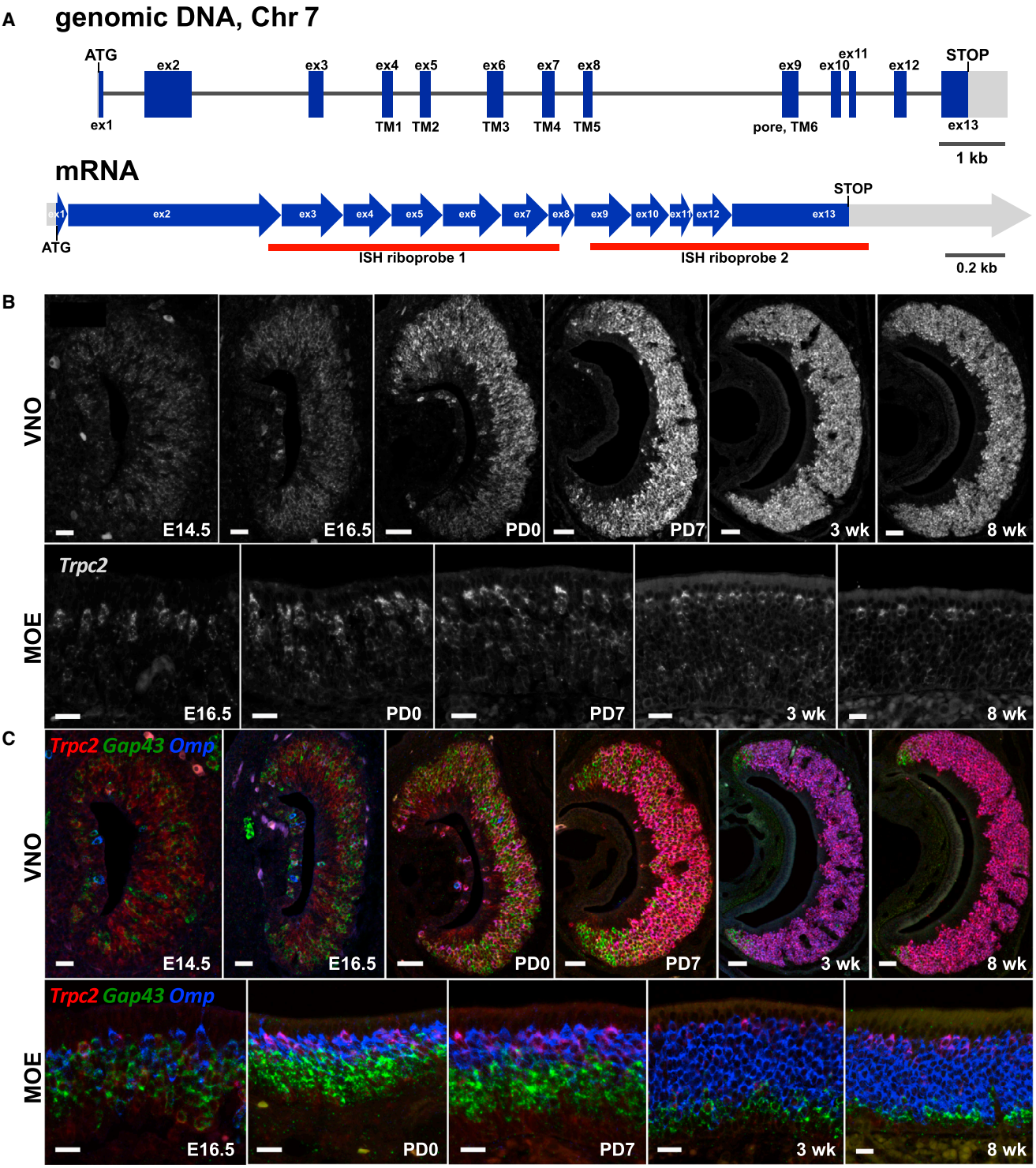


**Figure 1. The *Trpc2* Gene Is Expressed in the Mouse VNE and MOE at the RNA Level**

(A) Structure of the mouse *Trpc2* locus and its transcript consisting of 13 coding exons, with the extent of the two riboprobes used for ISH.

(B) Single-color ISH of the VNO and MOE with *Trpc2* ISH riboprobes 1+2 in C57BL/6 mice at various ages.

(C) Three-color ISH of the VNO and MOE with *Trpc2* ISH riboprobes 1+2, *Gap43*, and *Omp* in C57BL/6 mice at various ages. E, embryonic day; PD, postnatal day; wk, week.

Scale bars, 50 μm in images of the VNO at PD0, PD7, 3 wk, and 8 wk, and 20 μm in all other images.

acids. For ISH experiments, we designed two *Trpc2* riboprobes that span exons 3–8 (ISH riboprobe 1) or exons 9–13 (ISH riboprobe 2). We carried out single-color ISH (Figure 1B) and three-color ISH (Figure 1C) on coronal cryosections of the VNO and MOE of WT C57BL/6 mice at various ages, with both *Trpc2* riboprobes combined. In the VNE, *Trpc2* expression becomes detectable at or about embryonic day 14.5 (E14.5), initially in immature *Omp*− cells. After birth, there is an increase in the intensity of *Trpc2* ISH signal per cell and in the proportion and number of *Trpc2*+ cells in the VNE. At 8 weeks the VNE is strongly *Trpc2*+, except for the peripheral regions dorsally and ventrally, where neurogenesis takes place: the *Gap43*+ *Omp*− *Trpc2*− cells correspond to immature VSNs. In the MOE, *Trpc2* expression is detectable at or about E16.5, initially in *Gap43*+ *Omp*+ cells. After birth, *Trpc2* ISH signals become stronger in MOE cells and are readily detectable at 8 weeks, an adult age that is used for behavioral experiments. By RT-PCR and 5′ rapid amplification of cDNA ends (5′ RACE), we found that the major *Trpc2* transcript in the MOE is the same as in the VNO.

Next, we carried out a detailed ISH analysis of this previously unrecognized population of *Trpc2*+ MOE cells. We discovered that there are actually two types of *Trpc2*+ cells in the MOE, which can be distinguished by their location and gene-expression profile. These cells are abundantly present at 8 weeks (Figure 2). The first type of *Trpc2*+ MOE cells, which we refer to as type A cells, is scattered across the MOE, in both the dorsal (*Omacs*+ *Ocam*−) and ventral (*Omacs*− *Ocam*+) regions, as exemplified by box I in Figure 2A. Type A cell bodies typically occupy apical positions within the MOE, just under the sustentacular cell layer, and form a semicontinuous layer throughout the MOE. The second type of *Trpc2*+ MOE cells, which we refer to as type B cells, is confined to the lateralmost region of the MOE, as exemplified by box II in Figure 2A. The type B cell region is similar to the expression region of *MOR28* (*Olfr1507*), the most highly expressed OR gene (Khan et al., 2013). Type B cell bodies reside at all levels along the basal-to-apical dimension of the MOE. Interestingly, some type B cell bodies reside extremely apically, within the sustentacular cell layer. ISH for genes encoding components of the olfactory signal transduction pathway indicates that type A cells resemble canonical OSNs (Figures 2B and 2C). Type A cells are ISH+ for the cyclic-nucleotide gated channel subunit α2 (*Cnga2*), adenylate cyclase 3 (*Adcy3*), and the OSN-specific Gαolf gene (*Gnal*). Some type A cells express G protein subunit gene Gαo (*Gnao1*), and no cells express Gαi2 (*Gnai2*), as is the case for canonical OSNs. Type B cells express *Cnga2*, some cells express *Gnao1*, and no cells express *Gnai2*, in line with type A cells. What distinguishes type B from type A cells is that they are weakly or not positive for *Gnal*, and negative for *Adcy3* (Figure 2C). By three-color ISH with riboprobes for *Trpc2*, *Adcy3*, and *MOR28*, we counted 20,520 ± 1,269 SEM type B cells in the *MOR28*+ region of the MOE in three male C57BL/6 mice at 3 weeks. Counting type A cells will require stereological approaches, but we estimate that they number in the hundreds of thousands.

It is known that not all sensory neurons of the MOE are canonical OSNs. There are minor populations of MOE cells that express guanylate cyclase-D (*Gucy2d*) (Walz et al., 2007), inositol 1,4,5-triphosphate receptor 3/IP3R3 (*Itpr3*) and *Trpc6* (Elsaesser et al., 2005), or *Trpm5* (Hansen and Finger, 2008). Our ISH and IHC analyses indicate that type A and type B *Trpc2*+ MOE cells do not express any of these genes (data not shown).

Thus, the MOE of embryonic, postnatal, and adult WT C57BL/6 mice contains two types of cells that express *Trpc2* and have not been described previously. Type A and type B cells are distinguishable at the single-cell level by *Adcy3* expression (positive: type A; negative: type B).

## Trpc2 Protein Expression in the VNO and MOE of WT C57BL/6 Mice

To determine whether the *Trpc2* transcripts in MOE cells are translated into protein, we performed IHC with the same Trpc2 polyclonal antibody (Figure 3) that was used in the original report of Trpc2 expression in rat VSNs (Liman et al., 1999). In the VNO of mice at 3 weeks, Trpc2 signal is enriched along the apical border of the VNE (Figure 3A), which consists of VSN microvilli. This subcellular localization was an early indication of a role of Trpc2 in VSN chemosensory signal transduction (Liman et al., 1999; Menco et al., 2001). In the MOE of mice at various ages, Trpc2 signal is most prominent at the level of the cell bodies (Figure 3A). These IHC experiments confirm and extend the differences in intraepithelial location of cell bodies of type A cells (apical, just under the sustentacular layer) and type B cells (at all levels and also within the sustentacular cell layer). Whereas VSNs express the microvillous cell markers villin and espin, Trpc2+ MOE cells do not express these markers (Figure 3B and data not shown). The absence of villin expression is best appreciated in segments of the MOE where Trpc2+ cells are adjacent to members of the minor population of microvillous cells in the mouse MOE (Figure 3C; Rowley et al., 1989).

Western blotting reveals that the 2,673 bp *Trpc2-202* transcript, which contains only the coding sequence and encodes the predicted Trpc2 polypeptide of 890 amino acids, is translated into the predicted ~100 kDa band in transfected COS7 cells (Figure 3D). A band of similar size is obtained with crude membrane fractions from the whole olfactory mucosa (WOM) or the vomeronasal organ (VNO), and also with extracts from dorsal or lateral regions of the WOM separately. Consistent with the much smaller proportion of Trpc2+ cells in the MOE compared with the VNO, much more protein must be applied from WOM extracts to obtain band intensities similar to those achieved with the VNO extracts.

Thus, both RNA and protein are expressed from the *Trpc2* locus in the MOE of embryonic, postnatal, and adult WT C57BL/6 mice.

## Screening for Expression of Chemosensory Receptor Genes in *Trpc2*+ MOE Cells

In addition to the very large repertoire of OR genes, sensory neurons of the MOE and VNE express members of four gene repertoires encoding chemosensory G-protein-coupled receptors: vomeronasal receptor genes of type 1 (*Vmn1r*) or type 2 (*Vmn2r*), trace amine-associated receptor (*Taar*) genes, and formyl peptide receptor (*Fpr*) genes. We screened the MOE of WT C57BL/6 mice for chemosensory receptor gene expression with ISH riboprobes for members of these gene families, and

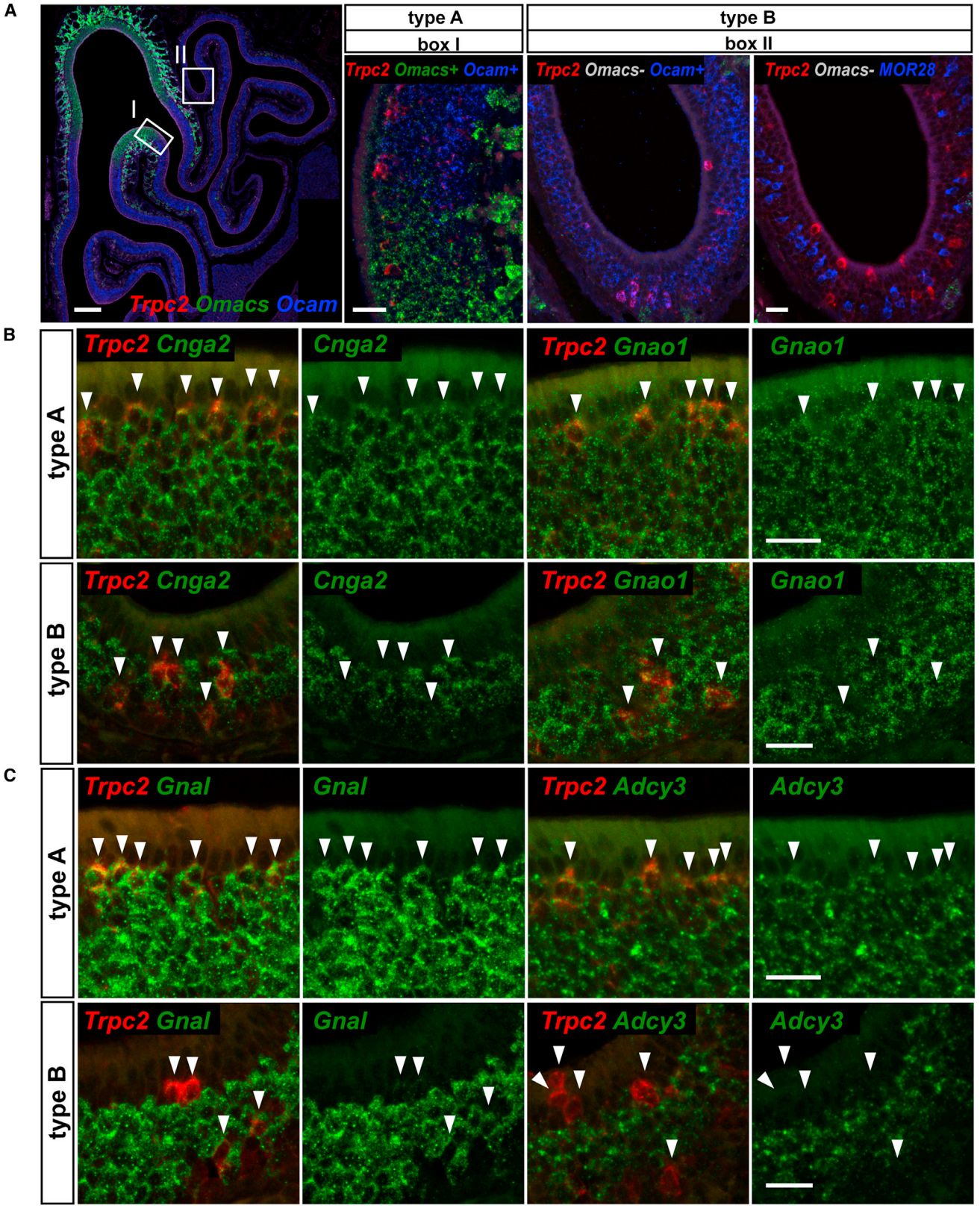


*(legend on next page)*

also for *Gucy2d* (Figure 4A). A few *Vmn1r*+ or *Vmn2r*+ cells have been reported in the MOE (Karunadasa et al., 2006; Pascarella et al., 2014). In three male 3-week-old C57BL/6 mice, we counted 40.67 ± 6.2 (SEM) cells labeled with a *V1rd* riboprobe mix; of these, 1 ± 0.58 were *Trpc2*+. In the same mice, we counted 26.67 ± 3.2 cells labeled with a *Vmn2r78* riboprobe, and 0.33 ± 0.33 of these were *Trpc2*+. These *Vmn1r*+ cells and *Vmn2r*+ cells may thus represent yet other, albeit very minor, cell types. *Trpc2*+ MOE cells do not express *Taar* genes or *Gucy2d* (Figure 4A), or *Fpr* genes (data not shown). No coexpression of *Trpc2* and a mix of five *class II OR* riboprobes (detecting seven genes) is observed (Figure 4B). The MOE region of the most highly expressed OR gene, the class II OR gene *MOR28* (*Olfr1507*), overlaps with the region of type B cells, but *MOR28*+ cells do not express *Trpc2* (Figure 4B). Interestingly, a mix of five *class I OR* riboprobes (detecting six genes) results in ISH colocalization with *Trpc2* in a fraction of type A cells (Figure 4B). When individual riboprobes from this mixture were tested, many cells that were labeled with the *Olfr69* riboprobe (recognizing also *Olfr68*, which has 97% nucleotide identity in the coding region) were labeled with *Trpc2* in mice at postnatal day 0, postnatal day 7, and 3 weeks (Figure 4C). In the same three C57BL/6 mice in which we counted cells labeled with the *V1rd* mix or *Vmn2r78*, we counted 1,286 ± 317 cells labeled with the *Olfr69* riboprobe; of these, 451.3 ± 121.8 (35.1%) were also labeled with *Trpc2*. We have not identified expression of members of the known chemosensory receptor gene families in type B cells.

Thus, with the caveat that the size and complexity of the chemosensory receptor gene families complicates the generality of conclusions about expression (in particular, about lack of expression), type A cells likely express a subset of the OR gene repertoire, of which *Olfr68/69* is the first example.

## A Trpc2-KO Strain Confirms the Specificity of ISH and IHC

The results described thus far were all obtained in WT C57BL/6 mice. The specificity of ISH and IHC reagents can be critically tested in gene knockout (KO) mice. We generated a Trpc2-KO strain by gene targeting in embryonic stem cells (ESCs). In this targeted mutation, the *pgk-neo* selectable marker replaces a 4.8 kb segment of genomic DNA comprising coding sequences of exons 9–13 that encode the pore region of the cation channel and transmembrane domain 6 (Figure 5A). This deletion mutant is an ideal negative control for ISH and IHC experiments. We examined homozygous mice and WT littermates that were backcrossed seven times to the 129/SvEv background. ISH riboprobe 2 is designed against exons 9–13 (Figure 1A), which are deleted in our Trpc2-KO mice. As expected, ISH with this riboprobe does not result in a signal in the VNO and MOE of Trpc2-KO mice (Figure 4B). The labeling pattern in WT mice (Figure 5B) is the same as that obtained with riboprobes 1 and 2 combined (Figures 1B and 1C), but riboprobe 2 alone gives a lower ISH signal than riboprobes 1 and 2 combined. Likewise, IHC with the Trpc2 polyclonal antibody does not show a signal in the VNO and MOE of Trpc2-KO mice (Figure 5C).

Thus, the negative control experiments with Trpc2-KO mice demonstrate the specificity of our observations of *Trpc2* expression at the RNA and protein levels in the MOE of WT C57BL/6 mice. Conversely, the absence of staining with this Trpc2 polyclonal antibody (Liman et al., 1999) in our Trpc2-KO mice confirms the specificity of this antibody in the mouse.

## A Trpc2-IRES-taulacZ Strain Enables Labeling of Axonal Projections

Our results thus far do not afford the conclusion that the type A and type B Trpc2+ MOE cells are neurons, although their gene expression profiles are similar to that of canonical OSNs. One criterion for these cells to be neurons is that, like canonical OSNs and VSNs, they extend axons that project to the olfactory bulb, where they coalesce into glomeruli. A classical technique for labeling mouse OSN or VSN axons is to generate a bicistronic knockin allele by gene targeting that results in coexpression of the protein encoded by the target gene with an axonal marker such as tauβ-galactosidase (Mombaerts et al., 1996). This genetic approach has been applied successfully to numerous OR genes (Mombaerts, 2006), *Vmn1r* genes (Belluscio et al., 1999; Rodriguez et al., 1999), *Vmn2r* genes (Del Punta et al., 2002; Ishii and Mombaerts, 2008, 2011; Leinders-Zufall et al., 2009), *Taar* genes (Pacifico et al., 2012), and *Gucy2d* (Walz et al., 2007).

We generated a Trpc2-IRES-taulacZ knockin by gene targeting in ESCs (Figure 6A). In this genetic design, the *Trpc2* coding region is not disrupted and intact Trpc2 protein is coexpressed with tauβ-galactosidase. The targeting frequency is extraordinarily high: 89% of G418-resistant ESC clones show Southern blot evidence for the targeted mutation. The VNE of Trpc2-IRES-taulacZ mice is labeled uniformly by IHC in sections (Figure 6B) and by X-gal histochemistry in whole mounts (Figure 6C), consistent with expression of Trpc2 by the overwhelming majority of VSNs. Labeled VSN axons course in several fascicles from the VNO along the septum of the nasal cavity, penetrate the cribriform plate, traverse across the medial surface of the main olfactory bulb, and terminate within glomeruli in the AOB at the posterior aspect of the main olfactory bulb (Figures 6B and

**Figure 2. Two Types of *Trpc2*+ Cells in the MOE**

(A) ISH of the MOE with riboprobes 1+2 *Trpc2*, for *Omacs*, *Ocam*, and *MOR28* in a C57BL/6 mouse at 8 weeks. *Trpc2*+ cells are scattered across the MOE and two areas are boxed. Box I straddles the *Omacs*+, *Ocam*− dorsal region of the MOE and the *Omacs*−, *Ocam*+ ventral region, and box II (*Omacs*−, *Ocam*+, *MOR28*+) is in the lateralmost region of the MOE. The location of *Trpc2*+ cell bodies differs in box I (mostly apical, just below the sustentacular cell layer; type A cells) compared with box II (all levels along the basal-to-apical dimension of the MOE, including within the sustentacular cell layer; type B cells).

(B) ISH with riboprobes 1+2 for *Trpc2* together with *Cnga2* or *Gnao1*. Both type A and type B cells express these genes, as do canonical OSNs. Arrowheads indicate cells that are colabeled.

(C) ISH with riboprobes 1+2 for *Trpc2* together with *Gnal* or *Adcy3*. Type B cells express *Gnal* weakly or not, and do not express *Adcy3* at all, in contrast to type A cells, which resemble canonical OSNs in this regard.

All mice were 8 weeks old. Scale bars, 200 μm for the left image in (A), and 20 μm in all other images.

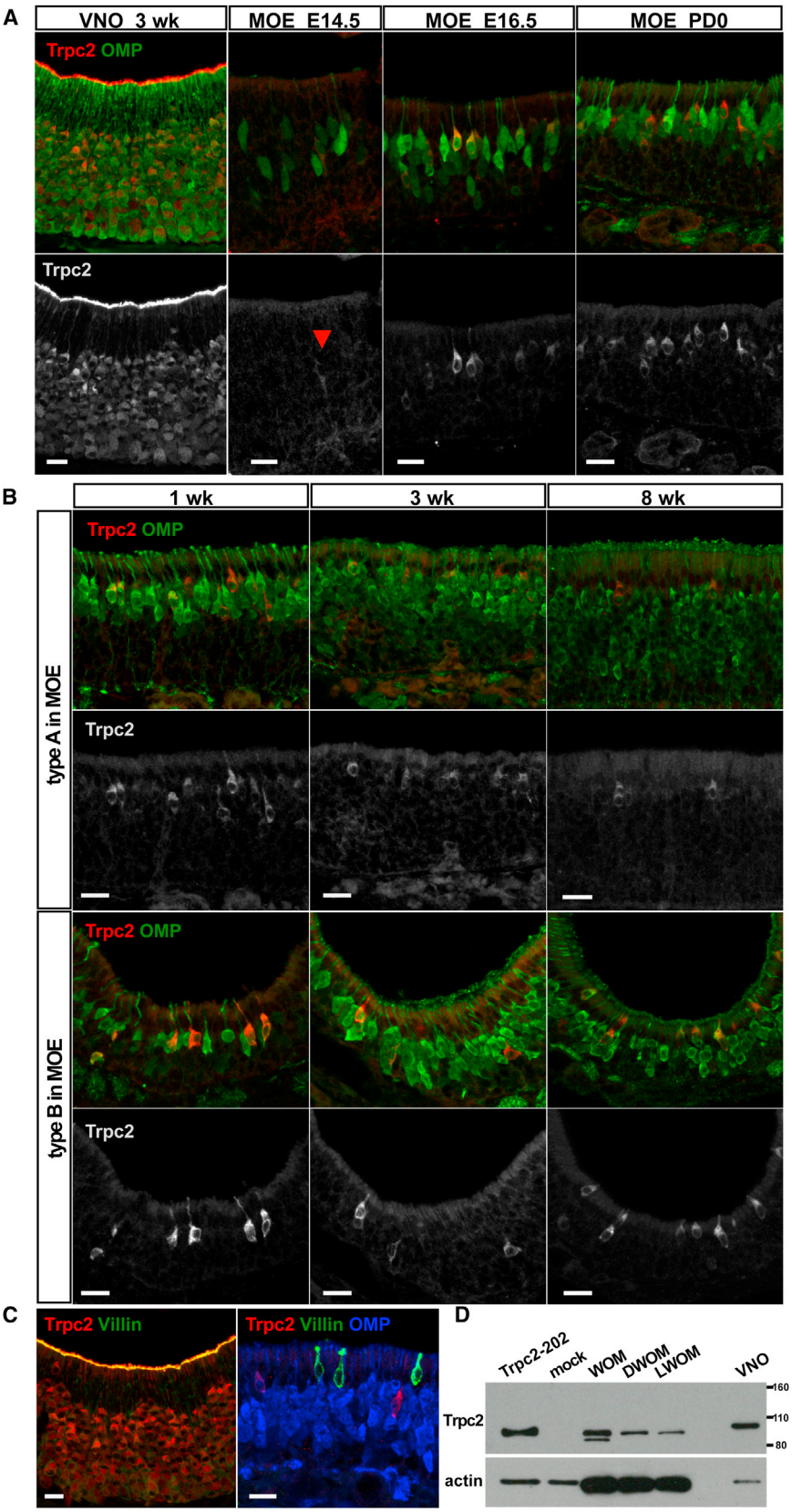


**Figure 3. Trpc2 Is Expressed in the Mouse VNE and MOE at the Protein Level**

(A) IHC of the VNO and MOE with a Trpc2 polyclonal antibody in C57BL/6 mice at various ages. Trpc2 immunoreactivity is enriched in VSN microvilli. In the MOE, Trpc2 immunoreactivity is present in a subset of cells and mostly in the cell bodies.

(B) Type A and type B cells differ in the location of their cell bodies along the basal-to-apical dimension of the MOE. Both cell types are readily detectable at 8 weeks.

(C) IHC of VNE (left) and MOE (right) sections with antibodies for the microvillous cell marker villin, Trpc2, and OMP in C57BL/6 mice (3 weeks). Villin immunoreactivity is abundantly present in VSN microvilli. There are villin-immunoreactive cells in the MOE, but Trpc2-immunoreactive MOE cells do not express villin.

(D) Western blot with Trpc2 antibody. A band of ~100 kDa is detected in lane Trpc2-202 (0.25 μg protein), a lysate from COS-7 cells that were transfected with a plasmid containing a Trpc2 cDNA. This band is not present in lysate from mock-transfected COS-7 cells. A band of similar size is obtained with crude membrane fractions from the whole olfactory mucosa (WOM, 20 μg), WOM dorsal region (DWOM, 20 μg), WOM lateral region (LWOM, 20 μg), and VNO (0.5 μg) of C57BL/6 mice (10 weeks). Actin serves as an internal control for protein content. The identity of the lower band in the WOM sample is not known. Scale bar, 20 μm.

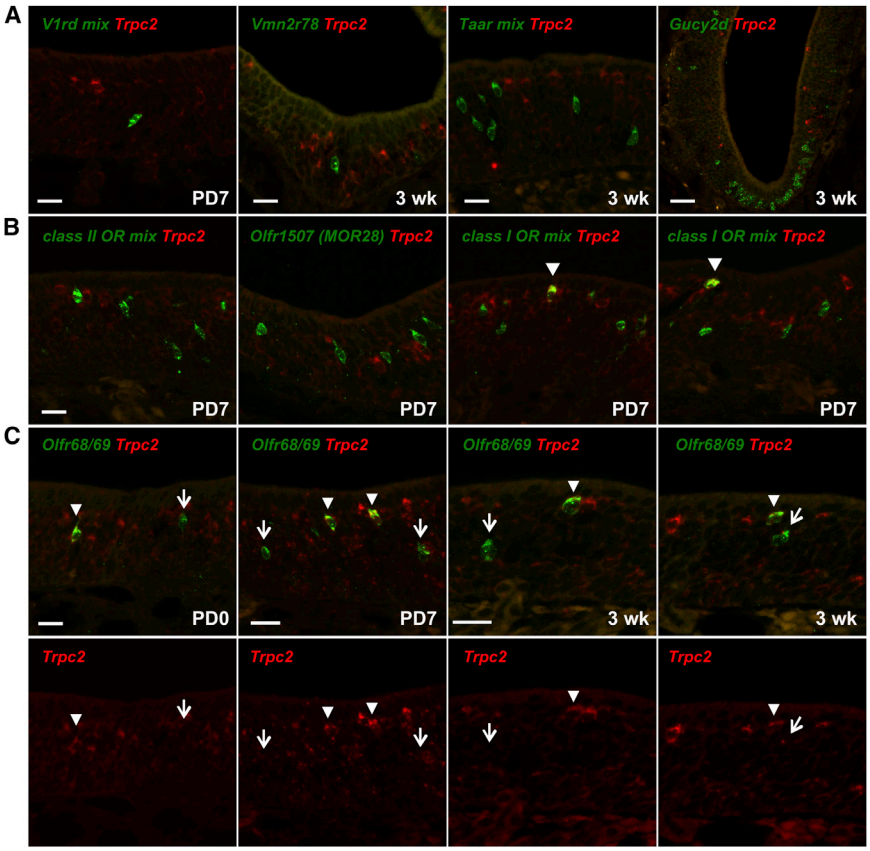


**Figure 4. Coexpression of *Trpc2*+ and *Olfr68/69* in Some MOE Cells**

Two-color ISH was performed to screen for expression of chemosensory receptor genes in *Trpc2*+ MOE cells in C57BL/6 mice at various ages.

(A) *Trpc2*+ cells are not labeled with a mix of riboprobes for *V1rd* genes (from the *Vmn1r* repertoire), *Vmn2r78*, a *Taar* mix, or *Gucy2d*.

(B) *Trpc2*+ cells are not labeled with riboprobes for a *class II OR* mix or *Olfr1507/MOR28*, but some cells are labeled with riboprobes for a *class I OR* mix. Arrowhead indicates a cell that is colabeled.

(C) Many (but not all) cells that are labeled with a riboprobe for the *Olfr68* and *Olfr69* genes are also labeled with the *Trpc2* riboprobe, and are type A cells. Arrowheads indicate cells that are colabeled and arrows indicate cells that are labeled with the *Olfr68/69* riboprobe, but not with the *Trpc2* riboprobe.

Scale bar, 20 μm.

6C). This mouse strain thus offers a convenient strategy to visualize VSNs and their axons coalescing into glomeruli within the AOB. The MOE of Trpc2-IRES-taulacZ mice contains scattered labeled cells representing type A or B cells (Figure 6D). The intensity of X-gal labeling is insufficient to visualize these MOE cells unambiguously in whole mounts.

In addition to all AOB glomeruli being labeled intensely, there are several labeled glomeruli in the main olfactory bulb of Trpc2-IRES-taulacZ mice (Figure 7). A few labeled glomeruli are located ventrally (Figure 7A) near the necklace glomeruli, a heterogeneous set of glomeruli that surround the AOB like a necklace and include Gucy2d+ glomeruli, which can be visualized in GC-D-IRES-taulacZ mice (Walz et al., 2007; Figure 7B). These labeled ventral glomeruli become apparent during the first postnatal week, and are still present at 1 year, in males and females (Figure 7C). The position of the labeled ventral glomeruli shows variability from mouse to mouse and from bulb to bulb. These glomeruli are immunoreactive for Cnga2 but negative for Adcy3 (Figure 7D), suggesting that they are formed by the coalescence of axons from type B cells in the MOE. In mice at 1 week, multiple glomeruli in the anteriormost part of the main olfactory bulb are innervated by labeled axons to various extents (Figure 7C). The identity of these glomeruli and axons remains to be clarified, but we suspect that some of these axons come from type A cells. When Trpc2-IRES-taulacZ mice are crossed with Cnga2-KO mice (Zheng et al., 2000), the pattern of labeled ventral (type B) glomeruli is disrupted in Cnga2 hemizygous males (Figure 7E); the number of glomeruli increases from 2.83 ± 0.31 (SEM; n = 6 bulbs) to 13.50 ± 1.19 (n = 4 bulbs; Figure 7F). Moreover, some of these glomeruli are located medially (1.75 ± 0.48, n = 4 bulbs) in Cnga2 hemizygous males instead of only ventrally on the surface of the bulb. Whereas the size of the AOB is similar in a Cnga2-KO background (Figure 7G), the main olfactory bulb of a Cnga2 hemizygous male is markedly smaller than that of a Cnga2 WT male, as can be evaluated readily by juxtaposing two half-brains (Figure 7H).

Thus, the Cnga2 expression, lack of Adcy3 expression, and Cnga2 dependence of the labeled ventral glomeruli suggest that type B cells in the MOE, but not VSNs, project their axons to these glomeruli.

## DISCUSSION

Here, we have extensively documented *Trpc2* gene and Trpc2 protein expression in the mouse MOE. We examined WT C57BL/6 mice, an inbred mouse strain that is widely used in chemosensory neuroscience research and is readily available. MOE expression has an embryonic onset, is not confined to a developmental time window, and persists in adulthood, when behavioral phenotypes are assessed. Reagent specificity is demonstrated by the absence of signals in Trpc2-KO mice. We find that there are two types of Trpc2+ MOE cells, termed A and B, which can be distinguished at the single-cell level by expression of *Adcy3* (positive: type A; negative: type B). These types can perhaps be subdivided further depending on more information about their gene expression profiles. Our initial analyses did not reveal expression of *Vmn1r*, *Vmn2r*, *Taar*, or *Gucyd2* in *Trpc2*+ MOE cells, with the caveat that the complexity and size of the *Vmn1r* and *Vmn2r* repertoires render such

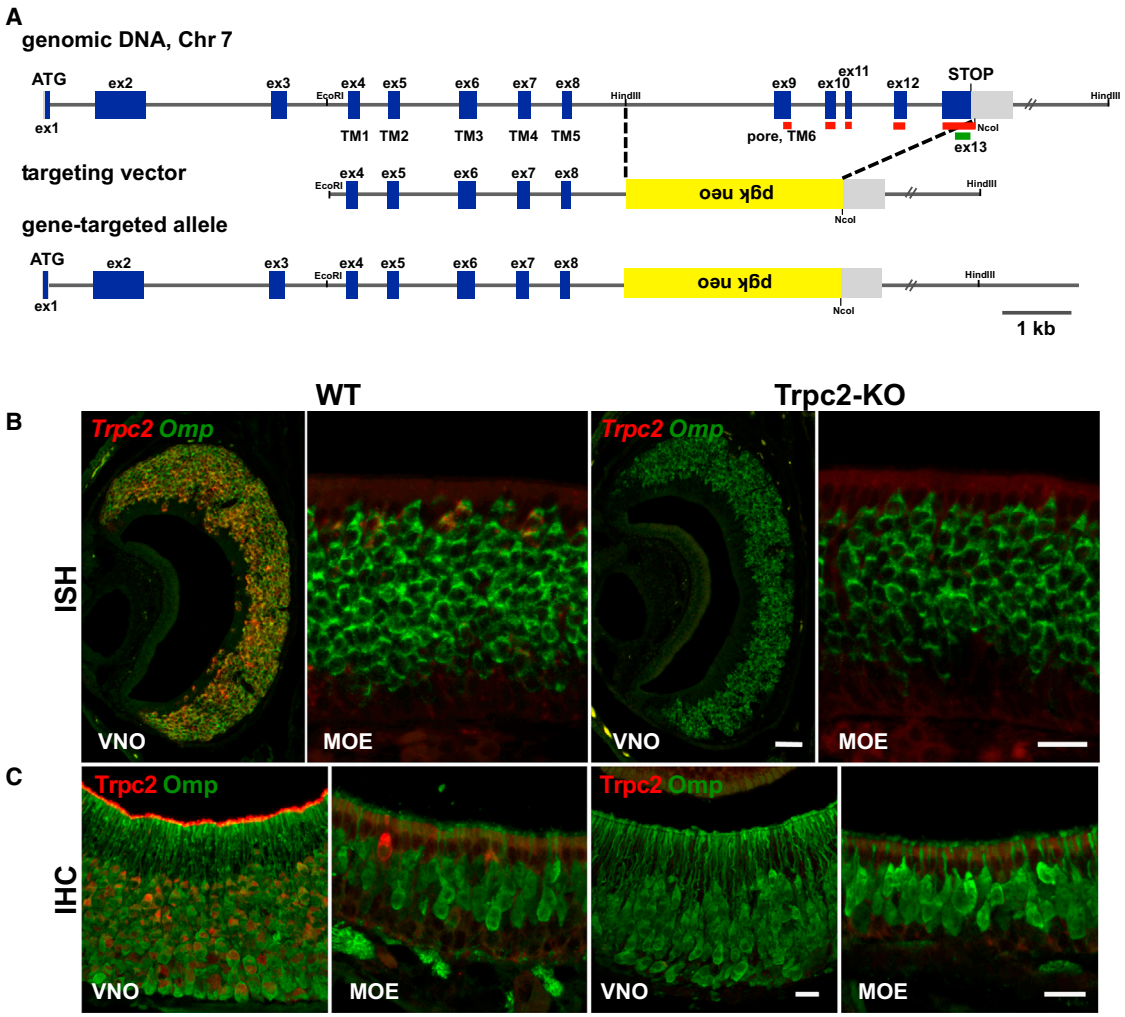


**Figure 5. Trpc2-KO Gene-Targeted Strain**

(A) Generation of a Trpc2-KO strain by gene targeting in ESCs. In the targeted mutation, the *pgk-neo* selectable marker replaces a 4.8 kb segment of genomic DNA comprising coding sequences of exons 9–13. Red bars indicate exons that are included in Trpc2 riboprobe 2. The green bar indicates the epitope of the Trpc2 polyclonal antibody.

(B) *Trpc2* signals with ISH riboprobe 2 are absent in sections of the VNO and MOE of a Trpc2-KO mouse (3 weeks). The WT mouse is a littermate in a 129/SvEv inbred background.

(C) Immunoreactive signals with a Trpc2 antibody are absent in sections of the VNO and MOE of a Trpc2-KO mouse (3 weeks). The WT mouse is a littermate in a 129/SvEv inbred background.

Scale bars, 50 μm in (B) for both VNO images, and 20 μm in all other images.

conclusions tentative. It is even more problematic to exclude or accurately describe the expression of the OR gene repertoire, due to its large size (~1,200 members). Our initial analyses did not reveal OR gene expression in type B cells. Approximately a third of *Olfr68*/*Olfr69*+ MOE cells express *Trpc2* and are type A cells. Because there are no odorous ligands or gene-targeted strains for these two class I OR genes, it is not possible to determine whether Trpc2 is required for chemosensory signaling in *Olfr68/69*+ *Trpc2*+ MOE cells. There is no reason to believe that our discovery of *Olfr68/69* coexpression with *Trpc2* was a stroke of luck, and we expect more examples of coexpression of *Trpc2* with OR genes to emerge. It will be particularly interesting to screen for expression of components of other chemosensory signaling pathways in type B cells. The coalescence of labeled axons into a few ventral glomeruli (Cnga2+ but Adcy3−) in Trpc2-IRES-taulacZ mice and the Cnga2 dependence of this coalescence pattern strongly suggest that these glomeruli are formed by axons from type B cells but not from VSNs, that Cnga2 provides an essential function in these cells, and that these cells are likely sensory neurons. Thus, Trpc2+ MOE cells represent (at least) two sensory neuronal cell types in the MOE, displaying hybrid gene expression profiles and properties between those of canonical OSNs and VSNs.

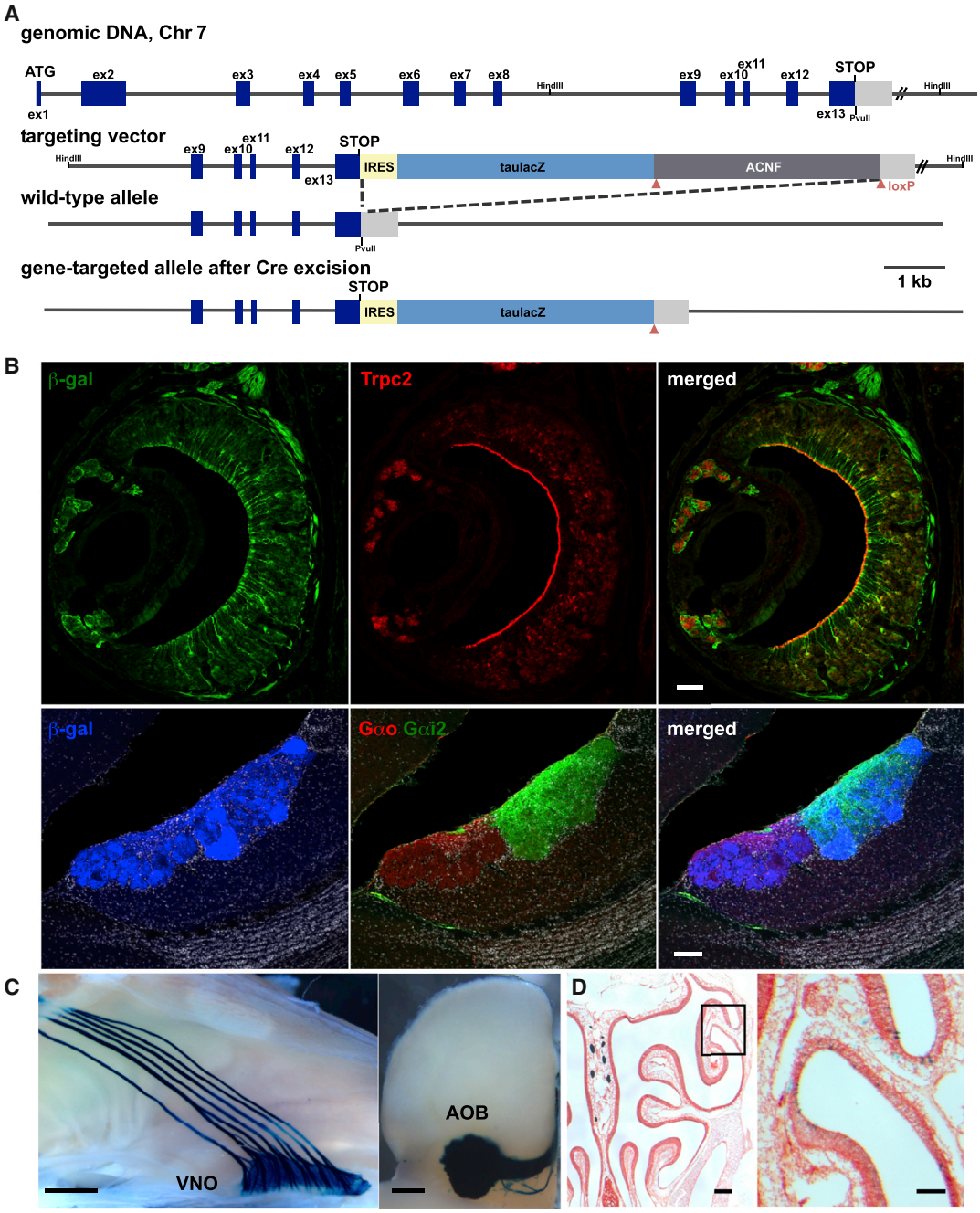


**Figure 6. Trpc2-IRES-taulacZ Gene-Targeted Knockin Strain**

(A) A knockin mutation, Trpc2-IRES-taulacZ, was generated by gene targeting in ESCs. The *IRES-taulacZ-ANCF* cassette was inserted after the stop codon of *Trpc2* by homologous recombination in ESCs. The *ACNF* cassette, a self-excising *neo* gene, was removed during transmission through the male germline, leaving a single *loxP* site (red triangle) behind in the locus. The *IRES* sequence allows for the cotranslation of intact Trpc2 with the axonal marker tauβ-galactosidase.

(B) IHC of sections of the VNO (top, 3 weeks) and AOB (bottom, 12 weeks) of a homozygous Trpc2-IRES-taulacZ mouse with antibodies against β-galactosidase and Trpc2 (VNO) or Gαo and Gαi2 (AOB). Immunoreactivity for β-galactosidase is present in cell bodies and axons, all the way to their glomeruli in the AOB. There is a sharp demarcation between the anterior part of the AOB (Gαi2) and the posterior part of the AOB (Gαo).

(C) Whole-mount staining of a homozygous Trpc2-IRES-taulacZ mouse at 10 weeks with the enzymatic substrate X-gal, which is converted into a blue precipitate. The left image shows a medial view of half of a mouse head: VNO and VSN axons are intensely labeled (4 hr incubation). The right image shows a dorsal view of the olfactory bulb: the AOB is uniformly and strongly labeled (24 hr incubation).

(D) X-gal staining of an MOE section of a homozygous Trpc2-IRES-taulacZ mouse at 4 weeks. The right image represents the box in the left image. Blue precipitates indicate type B cells (24 hr incubation).

Scale bars, 50 μm for (B) VNO, 100 μm for (B) AOB, 1 mm in (C), 200 μm in (D) left image, and 50 μm in (D) right image.

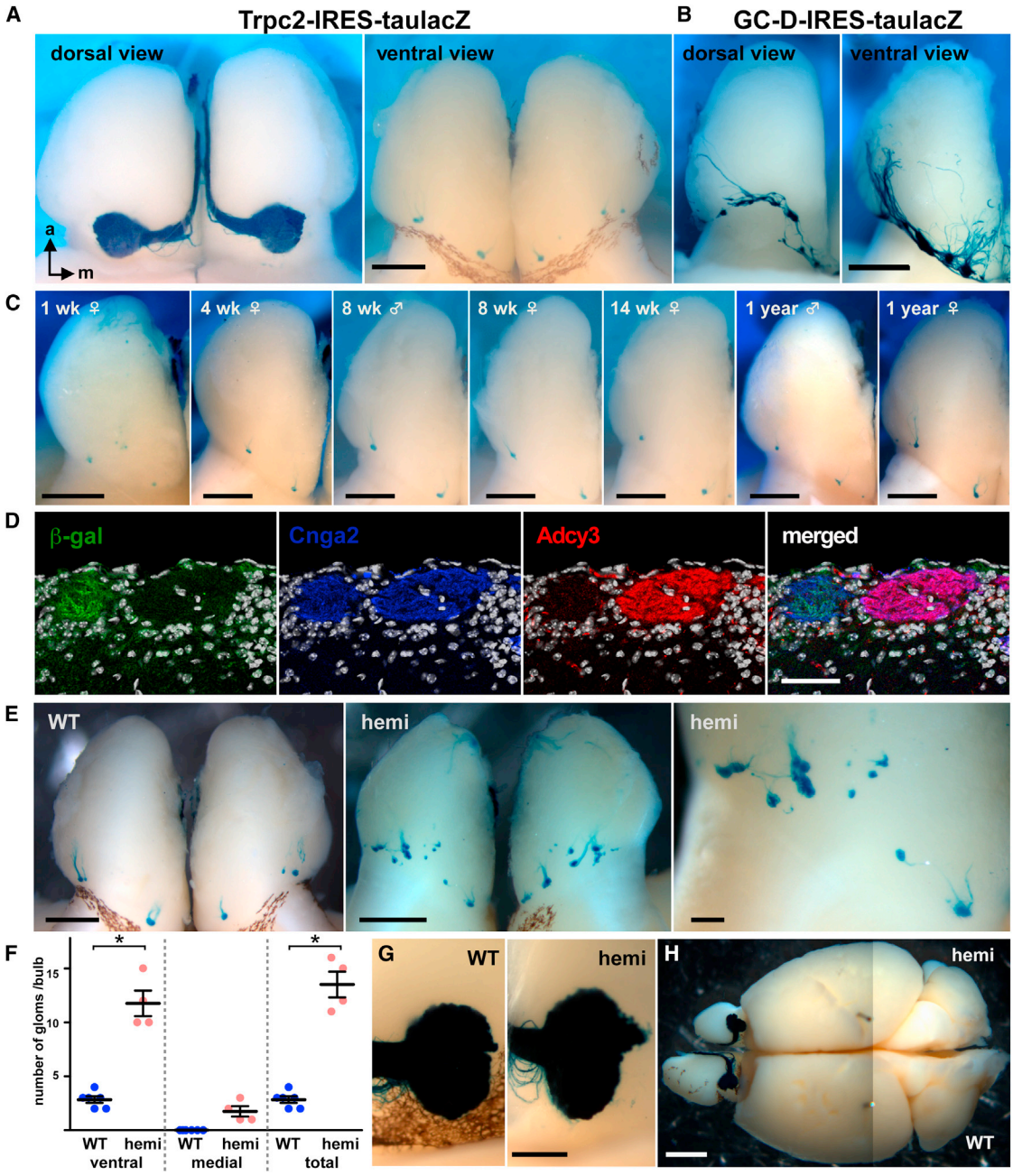


**Figure 7. Axonal Projections of Trpc2-Expressing Sensory Neurons to the Olfactory Bulb**

(A) Whole-mount X-gal staining of the olfactory bulbs of a homozygous Trpc2-IRES-taulacZ mouse at 8 weeks. The left panel shows a dorsal view: the vomeronasal nerves terminate dorsally (at the bottom) in the two AOBs. The right panel shows a ventral view: labeled axons form a few glomeruli ventrally in the posterior aspect of the main olfactory bulb. a, anterior; m, medial.

(B) Axonal projection patterns of Gucy2d-expressing cells in a homozygous GC-D-IRES-taulacZ mouse (Walz et al., 2007) at 13 weeks. These labeled glomeruli belong to the necklace glomeruli, which surround the AOB.

(C) Whole-mount ventral view of X-gal stained olfactory bulbs of homozygous Trpc2-IRES-taulacZ mice at various ages. Labeled ventral glomeruli are observed at all ages and in both sexes.

(D) IHC of ventral glomeruli with antibodies against β-galactosidase, Cnga2, and Adcy3. The left glomerulus is immunoreactive for β-galactosidase, positive for Cnga2 but negative for Adcy3, and is most likely formed by coalescence of type B axons. The adjacent right glomerulus is negative for β-galactosidase and positive for Cnga2 and Adcy3, and represents a typical glomerulus of the main olfactory bulb.

(E) Whole-mount ventral view of X-gal-stained olfactory bulbs of homozygous Trpc2-IRES-taulacZ male mice that are WT or hemizygous (hemi) for Cnga2-KO at 10 weeks. There are more labeled ventral glomeruli (type B) in hemizygous mice.

*(legend continued on next page)*

Optimized antigen retrieval methods and superresolution microscopy may reveal Trpc2 protein expression in dendrites and the presumptive cilia of Trpc2+ MOE cells. The demonstration of a ciliary subcellular localization of Trpc2 would suggest a functional role in chemosensory transduction. Screening for expression of members of large repertoires of chemosensory receptor genes (in particular, of OR genes) and components of other chemosensory signaling pathways in a heterogeneous cell population is a challenging task. To this end, one can apply genetic and molecular approaches such as high-throughput ISH analyses, generation of Trpc2 gene-targeted strains expressing a fluorescent marker, NanoString analyses from sorted cell populations (Khan et al., 2011), single-cell RT-PCR, and, ultimately, single-cell RNA sequencing. A gene-targeted strain expressing a fluorescent marker would also enable a functional analysis of Trpc2+ MOE cells, in order to characterize their electrophysiological properties and to screen for chemical ligands.

## Implications

According to conventional wisdom, Trpc2 expression is VSN specific in the mouse. Here, we used the same Trpc2 polyclonal antibody used to study rat VSNs (Liman et al., 1999) in order to document Trpc2 protein expression in the mouse MOE. Surprisingly, no evidence has been published that excludes *Trpc2* expression in the mouse MOE, but it turns out that such expression can be detected readily. This issue is critical because VSN-specific expression of Trpc2 in the mouse is obviously fundamental to the interpretation of the behavioral phenotypes of Trpc2-KO mice. Both male and female Trpc2-KO mice exhibit striking behavioral phenotypes, including the lack of male-male aggression and maternal aggression, and the appearance of male-male sexual behavior and male-like mounting behavior in females (Leypold et al., 2002; Stowers et al., 2002; Kimchi et al., 2007). Now we have found that Trpc2 is expressed not only in VSNs but also in MOE sensory neurons, including ~20,000 type B cells at 3 weeks. Importantly, these Trpc2+ MOE cells are not merely displaced or ectopic VSNs: the two Trpc2+ MOE cell types differ from canonical, *Vmn1r*- or *Vmn2r*-expressing VSNs in terms of gene expression profiles (such as *Cnga2* expression and lack of *Gnai2* expression), cellular features (no microvilli), and location of glomeruli in the main olfactory bulb. It is within the realm of possibility that other neuronal cell types in the mouse brain express Trpc2 as well (Elg et al., 2007; Boisseau et al., 2009), further challenging the VSN-specific interpretation of the behavioral phenotypes of Trpc2-KO mice. In addition, Trpc2 is expressed in nonneuronal cell types in the mouse (Löf et al., 2011; Hirschler-Laszkiewicz et al., 2012). Our Trpc2-IRES-taulacZ strain, which is publicly available from The Jackson Laboratory, will provide a convenient tool for examining Trpc2 expression histologically at the single-cell level throughout the body. We conclude that a continued VSN-specific interpretation of the behavioral phenotypes of Trpc2-KO mice awaits the classical test that these phenotypes can be reproduced in mice with a conditional, VSN-specific knockout of the *Trpc2* gene.

## EXPERIMENTAL PROCEDURES

### Generation of Mouse Strains with Gene-Targeted Mutations

A bacterial artificial chromosome containing *Trpc2*, 430d19, was isolated from RCPI-22, a 129S6/SvEvTac library (Children's Hospital Oakland Research Institute, Oakland, CA). To generate the targeting vector for the Trpc2-KO mutation, a 4.2 kb EcoRI-*HindIII* fragment was used for the left homology arm, and a 4.7 kb fragment composed of a *NcoI-HindIII* 0.5 kb fragment followed by a 4.2 kb HindIII fragment was used for the right homology arm. The selectable marker *pgk-neo* was inserted between the left and right arms. Homologous recombination creates a deletion of 4.8 kb of genomic DNA containing all *Trpc2* coding sequences, exons 9–13. The vector was linearized and electroporated into E14 ESCs as described previously (Mombaerts et al., 1996). Cells from the targeted ESC clone TRP116 were injected into C57BL/6 blastocysts and germline transmission was obtained. An inbred strain called Trpc2-KO (129SvEv-N7) was generated by seven backcrosses to 129SvEv. To generate the targeting vector for the Trpc2-IRES-taulacZ mutation, a 4.8 kb HindIII-*PvuII* fragment containing exons 9–13 of *Trpc2* was used for the left homology arm, and a 4.8 kb *PvuII-HindIII* fragment containing part of exon 13 was used for the right homology arm. A *PacI-AscI* site was generated at the *PvuII* site located 32 bp after the stop codon of *Trpc2*. The cassette *IRES-taulacZ-loxP-ACNF* was inserted into the newly generated *AscI* site. The vector was linearized and electroporated into E14 cells. Targeted ESC clones were injected into C57BL/6 blastocysts and chimeras were bred with WT C57BL/6 mice. A strain was established from targeted ESC clone B95. Mice were maintained in specified pathogen-free conditions in individually ventilated cages of the Tecniplast green line. Mouse experiments were carried out in accordance with NIH guidelines and the German Animal Welfare Act, European Communities Council Directive 2010/63/EU, and the institutional ethical and animal welfare guidelines of the Max Planck Institute of Biophysics and the Max Planck Research Unit for Neurogenetics. Approval was obtained from the IACUC of The Rockefeller University and the Veterinäramt of the City of Frankfurt. The following two strains are publicly available from The Jackson Laboratory: Trpc2-KO (129SvEv-N7) or 129S6.129P2-Trpc2<tm1Mom>/MomJ as JR#7890; and Trpc2-IRES-taulacZ in a mixed 129 × B6 genetic background or B6;129P2-Trpc2<tm3Mom>/MomJ as JR#6732.

### ISH and Cell Counting

ISH was performed as previously described (Ishii et al., 2004). For *Trpc2*, two riboprobes were combined in order to enhance the signal in WT mice: nt 2,012–2,999 from GenBank accession number NM_01644 (ISH riboprobe 1) and nt 3,131–4,068 (ISH riboprobe 2, deleted region in Trpc2-KO). The following riboprobes have been described previously: *OMP* and *GAP43* (Ishii et al., 2004); *Omacs* (Hirota et al., 2007); *Gnao1*, *Gnai2* (Ishii et al., 2003); *Gnal*, *Gnas*, *MOR7-1/Olfr578*, *MOR22-2/Olfr69*, *MOR32-4/Olfr672*, *MOR18-2/Olfr78*, *MOR23/Olfr16*, *MOR258-5/Olfr62*, *MOM101-1/Olfr520*, *MOR256-2P/Olfr819*, *MOR200-1/Olfr1031* (Omura et al., 2014); *MOR33-1/Olfr653* (Fuss et al., 2013); *MOR28/Olfr1507* (Fuss et al., 2007); and *Fpr* (Rivière et al., 2009) genes. We designed riboprobes for *Cnga2*, nt 2,042–2,997 from NM_007724; for *Adcy3*, nt 2,853–3,559 from NM_00115953; and for *Gucyd2*, nt 105–853 and 2,273–2,864 from NM_1130693. For the *V1rd* mix, three

(F) The number of labeled ventral glomeruli (type B) in Trpc2-IRES-taulacZ mice is increased in mice that are hemizygous for Cnga2-KO at 10 weeks. Asterisk indicates a p value < 0.01 in an unpaired t test. As no WT bulb has labeled medial glomeruli, statistics cannot be obtained for medial glomeruli.
(G) Whole-mount dorsal view of X-gal-stained AOBs of homozygous Trpc2-IRES-taulacZ male mice that are WT or hemizygous (hemi) for Cnga2-KO at 10 weeks. There is no difference in the size of the AOB.
(H) Dorsal view on the brain of homozygous Trpc2-IRES-taulacZ male mice that are WT (left half-brain) or hemizygous (right half-brain) for Cnga2-KO at 10 weeks. There is a striking difference in the size of the main olfactory bulb.
Scale bars, 1 mm in (A–C), 50 μm in (D), 1 mm in (E); 500 μm in (G), and 2 mm in (H).

riboprobes were synthesized: *V1rd7*, nt 436–1,296 from NM_030737 (detecting 11 *V1rd* genes), *V1rd12*, nt 1–864 from NM_206872 (detecting five *V1rd* genes), and *V1rd16*, nt 376–731 from NM_206869 (detecting 57 *V1rd* genes). The riboprobe *Vmn2r78* is nt 1,704–2,414 from NM_001105189.1 and should cross-hybridize to another 12 *Vnm2r* genes (*Vmn2r66*, *67*, *68*, *69*, *70*, *71*, *72*, *73*, *74*, *75*, *77*, *79*). For *Taar* genes, two mixes were used. The first mix consists of *Taar6* (nt 1–1,030 from NM_001010828.1) and *Taar7a* (nt 18–1,077 from NM_001010829), and should cross-hybridize to *Taar7b*, *7c*, *7d*, *7e*, *7f*. The second mix consists of *Taar2* (nt 1–960, from NM_001007266.1), *Taar3* (nt 1–1,010, from NM_001008429.1), *Taar4* (nt 1–10,044 from NM_001008499.1), *Taar5* (nt 1–1,014 from NM_001009574.1), *Taar8a* (nt 1–1,020 from NM_001010830.1, cross-hybridizing to *Taar8b*, *8c*), and *Taar9* (nt 1–1,047 from NM_001010831.1). Images were collected with a Zeiss LSM 710 confocal microscope. Some images of the VNO were flipped along a vertical axis so that all images in a panel would point in the same direction.

For counting of type B cells, three-color ISH was carried out with riboprobes for *Trpc2* (a mix of riboprobes 1 and 2), *Adcy3*, and *MOR28* on every fifteenth 12 μm section of the MOE of three C57BL/6 male mice at 3 weeks. MOE sections were analyzed from the beginning of the VNO to the posterior end of the nasal cavity. Images of *Trpc2*+ cells in the *MOR28*+ region were captured with a Zeiss LSM 710 confocal microscope. *Trpc2*+/*Adcy3*− cells in the *MOR28*+ region were classified as type B cells. A few immature type A cells in the region may have been included in these counts. The number of type B cells per mouse was estimated by multiplying the counts by 15. For colocalization ISH analysis with *Trpc2* and *Olfr69*, *V1rd* mix, or *Vmn2r78*, cells were counted in every fifteenth MOE section of three C57BL/6 male mice at 3 weeks. All images of chemoreceptor-positive cells were taken as single shots at the sharpest focus point or by the z-stack mode.

### IHC and X-Gal Histochemistry

For IHC, mice were anesthetized by injection of ketamine HCl and xylazine (150 mg/kg and 10 mg/kg body weight, respectively) and perfused with ice-cold PBS, followed by 4% PBS in PBS. The mouse heads were dissected, postfixed in 4% paraformaldehyde (PFA), and decalcified in 0.45 M EDTA in 1× PBS overnight at 4°C. Samples were cryoprotected in 15% and 30% sucrose in 1× PBS at 4°C, frozen in O.C.T. Compound (Tissue-Tek), and sectioned at 12 μm with a Leica CM3500 cryostat. Sections were washed with 1× PBS and, if necessary, antigen retrieval treatment was applied with 10 mM citric buffer (pH 6.0) or 10 mM Tris buffer (pH 9.5). Washed sections were blocked with 10% normal goat serum or normal donkey serum, 0.1% Triton X-100 in 1× PBS for 1 hr at room temperature. After the blocking step, sections were incubated in 3% BSA, 0.1% Triton X-100 in 1× PBS for overnight at 4°C with the following primary antibodies: rabbit anti-Trpc2 (1:500; Liman et al., 1999), goat anti-OMP (1:1,000; Wako Chemicals), mouse anti-iP3 receptor type 3 (1:1,000; BD Transduction Laboratories), mouse anti-villin (1:600; Chemicon), chicken anti-β-galactosidase (1:500; Abcam), mouse anti-Gαi2 (1:500; Millipore), rabbit anti-Gαo (1:500; Santa Cruz Biotechnology), rabbit anti-AC III (1:1,000; Santa Cruz Biotechnology), and goat anti-Cnga2 (1:300; Santa Cruz Biotechnology). After incubation with primary antibodies, sections were incubated with secondary antibodies for 1.5 hr at room temperature. For sections of the olfactory bulb, nuclear staining was done with DAPI (1:10,000; Molecular Probes) after the washing steps. Sections were analyzed with a Zeiss LSM 710 confocal microscope. X-gal histochemistry was performed as previously described (Mombaerts et al., 1996) except that tissues were fixed in 4% PFA in 1× PBS without $MgSO_4$ and EGTA. Images of X-gal-stained whole mounts were taken under a Zeiss Stemi SV11 stereomicroscope with an AxioCam and AxioVision LE software.

### Western Blotting

Crude membrane fractions were extracted from the VNO and WOM of C57BL/6 mice (10 weeks old). The crude membrane fractions were analyzed in parallel with cell lysate of COS-7 cells in which either a plasmid with a Trpc2 cDNA or the mock plasmid pCMV-Tag4B (Stratagene) was transfected by using the NuPAGE system (Invitrogen). Rabbit anti-Trpc2 (1:3,000, Liman et al., 1999, a gift from Emily Liman) and mouse anti-actin (1:7,500; Millipore) were used as primary antibodies. Horseradish peroxidase-conjugated secondary antibodies were applied and immunoreactive protein bands were visualized with a chemiluminescence reaction kit (ECL Prime Western Blotting Detection reagent; GE Healthcare).

## ACKNOWLEDGMENTS

The authors thank Emily Liman for the crucial gift of the Trpc2 antibody; Paul Feinstein for generating the Trpc2-KO strain in the laboratory of P.M. at The Rockefeller University, and for plasmids containing the *Trpc2* locus to generate the Trpc2-IRES-taulacZ targeting vector; Wei Tang for blastocyst injections; Ivan Rodriguez for *Fpr* riboprobe plasmids; Tobias Burbach for technical assistance; and Bolek Zapiec for help with figure artwork. P.M. received grant support from ERC Advanced Grant ORGENECHOICE and generous support from the Max Planck Society.

Received: April 21, 2014
Revised: May 30, 2014
Accepted: June 9, 2014
Published: July 3, 2014

## REFERENCES

Belluscio, L., Koentges, G., Axel, R., and Dulac, C. (1999). A map of pheromone receptor activation in the mammalian brain. Cell *97*, 209–220.

Boisseau, S., Kunert-Keil, C., Lucke, S., and Bouron, A. (2009). Heterogeneous distribution of TRPC proteins in the embryonic cortex. Histochem. Cell Biol. *131*, 355–363.

Del Punta, K., Puche, A., Adams, N.C., Rodriguez, I., and Mombaerts, P. (2002). A divergent pattern of sensory axonal projections is rendered convergent by second-order neurons in the accessory olfactory bulb. Neuron *35*, 1057–1066.

Dulac, C., and Torello, A.T. (2003). Molecular detection of pheromone signals in mammals: from genes to behaviour. Nat. Rev. Neurosci. *4*, 551–562.

Dulac, C., and Wagner, S. (2006). Genetic analysis of brain circuits underlying pheromone signaling. Annu. Rev. Genet. *40*, 449–467.

Elg, S., Marmigere, F., Mattsson, J.P., and Ernfors, P. (2007). Cellular subtype distribution and developmental regulation of TRPC channel members in the mouse dorsal root ganglion. J. Comp. Neurol. *503*, 35–46.

Elsaesser, R., Montani, G., Tirindelli, R., and Paysan, J. (2005). Phosphatidylinositide signalling proteins in a novel class of sensory cells in the mammalian olfactory epithelium. Eur. J. Neurosci. *21*, 2692–2700.

Fraser, E.J., and Shah, N.M. (2014). Complex chemosensory control of female reproductive behaviors. PLoS One *9*, 2:e90368.

Fuss, S.H., Omura, M., and Mombaerts, P. (2007). Local and cis effects of the H element on expression of odorant receptor genes in mouse. Cell *130*, 373–384.

Fuss, S.H., Zhu, Y., and Mombaerts, P. (2013). Odorant receptor gene choice and axonal wiring in mice with deletion mutations in the odorant receptor gene SR1. Mol. Cell. Neurosci. *56*, 212–224.

Hansen, A., and Finger, T.E. (2008). Is TrpM5 a reliable marker for chemosensory cells? Multiple types of microvillous cells in the main olfactory epithelium of mice. BMC Neurosci. *9*, 115.

Hirota, J., Omura, M., and Mombaerts, P. (2007). Differential impact of Lhx2 deficiency on expression of class I and class II odorant receptor genes in mouse. Mol. Cell. Neurosci. *34*, 679–688.

Hirschler-Laszkiewicz, I., Zhang, W., Keefer, K., Conrad, K., Tong, Q., Chen, S.J., Bronson, S., Cheung, J.Y., and Miller, B.A. (2012). Trpc2 depletion protects red blood cells from oxidative stress-induced hemolysis. Exp. Hematol. *40*, 71–83.

Ishii, T., and Mombaerts, P. (2008). Expression of nonclassical class I major histocompatibility genes defines a tripartite organization of the mouse vomeronasal system. J. Neurosci. *28*, 2332–2341.

Ishii, T., and Mombaerts, P. (2011). Coordinated coexpression of two vomeronasal receptor V2R genes per neuron in the mouse. Mol. Cell. Neurosci. *46*, 397–408.

Ishii, T., Hirota, J., and Mombaerts, P. (2003). Combinatorial coexpression of neural and immune multigene families in mouse vomeronasal sensory neurons. Curr. Biol. *13*, 394–400.

Ishii, T., Omura, M., and Mombaerts, P. (2004). Protocols for two- and three-color fluorescent RNA in situ hybridization of the main and accessory olfactory epithelia in mouse. J. Neurocytol. *33*, 657–669.

Karunadasa, D.K., Chapman, C., and Bicknell, R.J. (2006). Expression of pheromone receptor gene families during olfactory development in the mouse: expression of a V1 receptor in the main olfactory epithelium. Eur. J. Neurosci. *23*, 2563–2572.

Khan, M., Vaes, E., and Mombaerts, P. (2011). Regulation of the probability of mouse odorant receptor gene choice. Cell *147*, 907–921.

Khan, M., Vaes, E., and Mombaerts, P. (2013). Temporal patterns of odorant receptor gene expression in adult and aged mice. Mol. Cell. Neurosci. *57*, 120–129.

Kimchi, T., Xu, J., and Dulac, C. (2007). A functional circuit underlying male sexual behaviour in the female mouse brain. Nature *448*, 1009–1014.

Leinders-Zufall, T., Ishii, T., Mombaerts, P., Zufall, F., and Boehm, T. (2009). Structural requirements for the activation of vomeronasal sensory neurons by MHC peptides. Nat. Neurosci. *12*, 1551–1558.

Leypold, B.G., Yu, C.R., Leinders-Zufall, T., Kim, M.M., Zufall, F., and Axel, R. (2002). Altered sexual and social behaviors in trp2 mutant mice. Proc. Natl. Acad. Sci. USA *99*, 6376–6381.

Liman, E.R., Corey, D.P., and Dulac, C. (1999). TRP2: a candidate transduction channel for mammalian pheromone sensory signaling. Proc. Natl. Acad. Sci. USA *96*, 5791–5796.

Löf, C., Viitanen, T., Sukumaran, P., and Törnquist, K. (2011). TRPC2: of mice but not men. Adv. Exp. Med. Biol. *704*, 125–134.

Menco, B.P., Carr, V.M., Ezeh, P.I., Liman, E.R., and Yankova, M.P. (2001). Ultrastructural localization of G-proteins and the channel protein TRP2 to microvilli of rat vomeronasal receptor cells. J. Comp. Neurol. *438*, 468–489.

Mombaerts, P. (2006). Axonal wiring in the mouse olfactory system. Annu. Rev. Cell Dev. Biol. *22*, 713–737.

Mombaerts, P., Wang, F., Dulac, C., Chao, S.K., Nemes, A., Mendelsohn, M., Edmondson, J., and Axel, R. (1996). Visualizing an olfactory sensory map. Cell *87*, 675–686.

Omura, M., Grosmaitre, X., Ma, M., and Mombaerts, P. (2014). The β2-adrenergic receptor as a surrogate odorant receptor in mouse olfactory sensory neurons. Mol. Cell. Neurosci. *58*, 1–10.

Pacifico, R., Dewan, A., Cawley, D., Guo, C., and Bozza, T. (2012). An olfactory subsystem that mediates high-sensitivity detection of volatile amines. Cell Reports *2*, 76–88.

Papes, F., Logan, D.W., and Stowers, L. (2010). The vomeronasal organ mediates interspecies defensive behaviors through detection of protein pheromone homologs. Cell *141*, 692–703.

Pascarella, G., Lazarevic, D., Plessy, C., Bertin, N., Akalin, A., Vlachouli, C., Simone, R., Faulkner, G.J., Zucchelli, S., Kawai, J., et al. (2014). NanoCAGE analysis of the mouse olfactory epithelium identifies the expression of vomeronasal receptors and of proximal LINE elements. Front. Cell. Neurosci. *8*, 41.

Rivière, S., Challet, L., Fluegge, D., Spehr, M., and Rodriguez, I. (2009). Formyl peptide receptor-like proteins are a novel family of vomeronasal chemosensors. Nature *459*, 574–577.

Rodriguez, I., Feinstein, P., and Mombaerts, P. (1999). Variable patterns of axonal projections of sensory neurons in the mouse vomeronasal system. Cell *97*, 199–208.

Rowley, J.C., 3rd, Moran, D.T., and Jafek, B.W. (1989). Peroxidase backfills suggest the mammalian olfactory epithelium contains a second morphologically distinct class of bipolar sensory neuron: the microvillar cell. Brain Res. *502*, 387–400.

Stowers, L., Holy, T.E., Meister, M., Dulac, C., and Koentges, G. (2002). Loss of sex discrimination and male-male aggression in mice deficient for TRP2. Science *295*, 1493–1500.

Walz, A., Feinstein, P., Khan, M., and Mombaerts, P. (2007). Axonal wiring of guanylate cyclase-D-expressing olfactory neurons is dependent on neuropilin 2 and semaphorin 3F. Development *134*, 4063–4072.

Wu, Z., Autry, A.E., Bergan, J.F., Watabe-Uchida, M., and Dulac, C.G. (2014). Galanin neurons in the medial preoptic area govern parental behaviour. Nature *509*, 325–330.

Wyatt, T.D. (2014). Pheromones and Animal Behavior (New York: Cambridge University Press).

Zheng, C., Feinstein, P., Bozza, T., Rodriguez, I., and Mombaerts, P. (2000). Peripheral olfactory projections are differentially affected in mice deficient in a cyclic nucleotide-gated channel subunit. Neuron *26*, 81–91.